Phase separation phenomenon and mechanism in the preparation of cast stone from liquid slag from phosphorus-smelting furnace

QIUYU ZHANG[a], JUN ZHOU[a,*], ZHU SHU[a], TIANTIAN LI[a], YANXIN WANG[b]
[a]*Engineering Research Center of Nano-Geomaterials of Ministry of Education & Faculty of Material Science and Chemistry, China University of Geosciences, 430074 Wuhan, P. R. China*
[b]*School of Environmental Studies, China University of Geosciences, 430074 Wuhan, P. R. China*

A novel approach of preparing cast stone directly from hot liquid phosphorus slag (PS) discharged from phosphorus-smelting furnace had been proposed and tested in the previous work. In this paper, the phase separation behavior and phenomenon occurred during heat-treating the precursor into cast stone products were systematically observed and analyzed by XRD, FESEM and EDAX techniques. Combining some classical theory of phase separation with the measured results, it can be deduced that, the phase separation is mainly governed by the mechanism of binodal decomposition, and the growth of the separated droplets primarily conforms to the theory of Ostwald ripening. This study contributes a theoretical foundation to the preparation of the PS cast stones.

(Received July 2, 2013; accepted March 13, 2014)

Keywords: Phosphorus slag, Cast stone, Phase separation, Binodal decomposition, Ostwald ripening

1. Introduction

In the last decades, the phosphorus slag (PS) has attracted an interesting attention due to the strong application potential in the construction materials. PS is a liquid waste by-product with the temperature of 1300-1500 °C, discharged from phosphorus-smelting electric furnace during elemental phosphorus production [1]. Generally, the hot liquid PS is water-quenched into solid grains and then land-filled or used as a start material in the production of cement, concrete, glass-ceramics and so on [2-5].

Recently, in order to simultaneously recycle substance and enormous heat energy contained in the PS, a novel technique of directly using the hot liquid PS to prepare cast stone had been proposed and studied by the authors [6]. In this technique, the modified liquid PS was cast into glassy parent panels (precursor) and subsequently heat-treated at 900 °C for 1 h to obtain cast stone (named as *PS cast stone*) after annealing. The obtained cast stone has a high bending strength and a bright and opalescent appearance, and can be used as decorative building materials.

During heat-treating the precursor, the most important physicochemical phenomenon is the transformation of the transparent state of the precursor into an opalescent one of the cast stone, indicating that the precursor underwent phase separation. Therefore, a key theoretical work of developing the cast stone from the hot liquid PS should focus on the exploration of phase separation phenomenon and mechanism basing on their specific chemical composition.

In this research, the major objective is to systematically investigate the phase separation phenomenon and mechanism in the course of heat-treating the precursor into the cast stone, based on the classical theory of phase separation and the characteristics of the PS cast stone and its precursor measured by XRD, FESEM and EDAX.

2. Experimental

Water-quenched PS grains were obtained from an elemental phosphorus production company in Guizhou province, China, and its chemical composition was shown in Table 1. The cast stone samples were prepared based on the technique proposed by Zhou et al [6]. 76 wt% PS grains were remelted into the liquid at 1400 °C for 0.5 h in a corundum crucible; meanwhile, 18 wt% quartz powder and 6 wt% calcined kaolinitic clay, as the modifying materials, were preheated at 1000 °C. Subsequently, the pretreated modifying materials were poured into the liquid PS, and then co-melted at 1450 °C for 1 h to obtain modified liquid PS, and finally were cast and quickly quenched into the precursor of cast stone.

The precursor presents a transparent glass state and its chemical composition is given in Table 2.

In order to explore the phase separation phenomenon and mechanism during the precursor being heat-treated into the cast stone, the precursors were heat-treated at 900 °C for the variable time of 0.5 h, 1 h, 2 h, 4 h, 8 h, 14 h and 24 h, and after naturally annealing, the opalescent cast stone samples were obtained and labeled as T-0.5, T-1, T-2, T-4, T-8, T-14 and T-24, respectively.

The qualitative determination of phase composition of the precursor and cast stone specimens were analyzed by the X-ray Diffractometer (XRD; D/Max-3B, Rigaku), with Cu Kα radiation, at 35kV and 40 mA with 10 s scanning time. The microstructures of the precursor and cast stone specimens were characterized using Field Emission Scanning Electron Microscope (FESEM; FEI Quanta450 FEG), and the micro-area element composition of the cast stone T-8 was measured by Energy Dispersive Analysis of X-ray (EDAX) equipped in FESEM. Prior to the FESEM and EDAX measurements, all specimens were polished and etched in the HF solution of 5 % for 1 min at room temperature and coated with a thin layer of carbon.

3. Results

3.1 Determination of phase composition

The XRD patterns of precursor and cast stone samples were displayed in Fig. 1. The XRD patterns of the precursor and cast stone samples heat-treated for 0.5-14 h don't display any crystalline peaks, but broad humps are observed in the range of 20-40°, indicating these specimens are all amorphous. When the heat-treating time extends to 24 h, some weak diffraction peaks attributed to β-wollastonite appear, signifying that the precursor has the propensity to crystallize after the full phase separation.

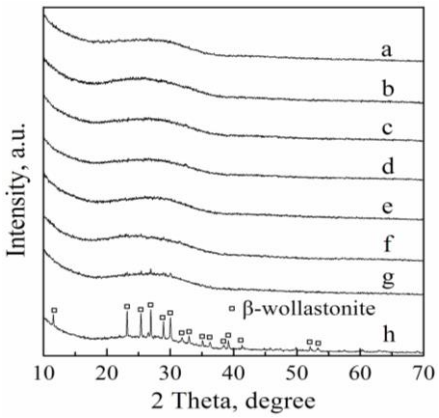

Fig. 1. XRD patterns of (a) precursor and cast stone samples (b) T-0.5, (c) T-1, (d) T-2, (e) T-4, (f) T-8, (g) T-14 and (h) T-24.

Table 1. The chemical composition (wt%) of the phosphorus slag.

Chemical component	SiO_2	Al_2O_3	TFe_2O_3	MgO	CaO	Na_2O	K_2O	P_2O_5	F
Composition	41.12	5.05	0.17	0.79	46.53	0.29	0.68	2.93	2.22

Table 2. The chemical composition (wt%) of the precursor of cast stone.

Chemical component	SiO_2	Al_2O_3	TFe_2O_3	MgO	CaO	Na_2O	K_2O	P_2O_5	F
Composition	55.22	8.32	0.48	0.82	30.23	0.25	0.68	2.31	1.69

3.2 Change of microstructure with heat-treating time

The microstructures of the precursor and cast stone samples were shown in Fig. 2. The micrograph of precursor exhibits a typical vitreous microstructure (Fig. 2a), which corresponds to the macroscopically optically transparent appearance of the precursor. In contrast, the images of cast stone samples present a great amount of micron-size droplets with the sizes of 0.06-0.70 μm in the glassy matrix, combining with their amorphous nature determined by XRD, indicating that the glass-in-glass phase separation occurred during heat-treating the precursor into cast stone. Obviously, the precipitation of the droplets in the course of phase separation results in the macroscopically opalescent appearance of the as-prepared cast stone.

For the FESEM image of each cast stone, a total of 350 droplets were randomly selected and their diameters were statistically analyzed using *Nano measurer* software.

The size distribution and mean diameter of the droplets are shown respectively in Fig. 3 and Fig. 4. It can be found that the size distributions of the droplets in various cast stones conform to a normal distribution, and the size distribution ranges become wide and the mean diameter increases with the increase of the heat-treating time. On the other hand, it can be discovered that the number of droplets per unit area (droplet distribution density) is inversely correlated with the heat-treating time, as shown in Fig. 5.

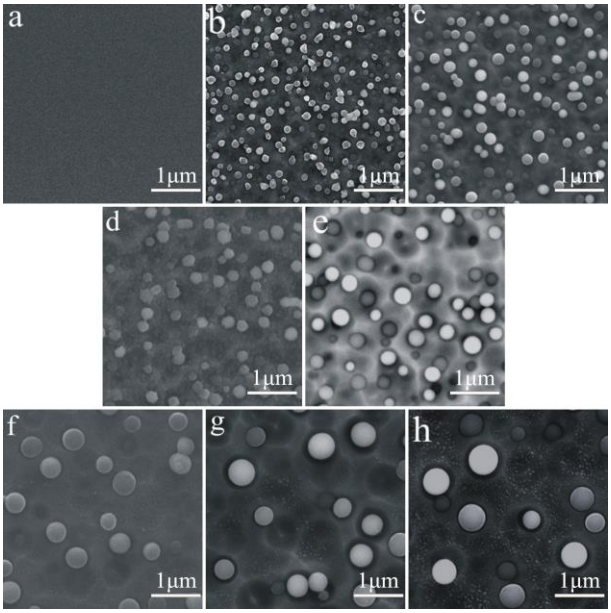

Fig. 2. FESEM images of (a) precursor and cast stone samples (b) T-0.5, (c) T-1, (d) T-2, (e) T-4, (f) T-8, (g) T-14 and (h) T-24.

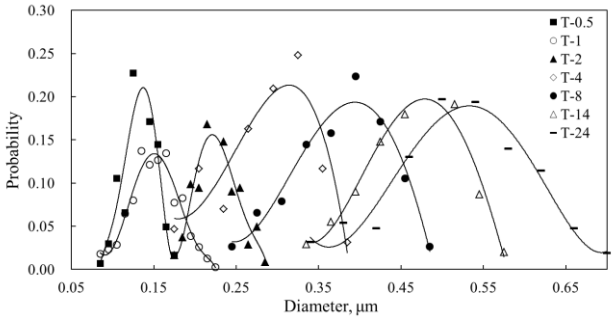

Fig. 3. The size distributions of the droplets in cast stone samples.

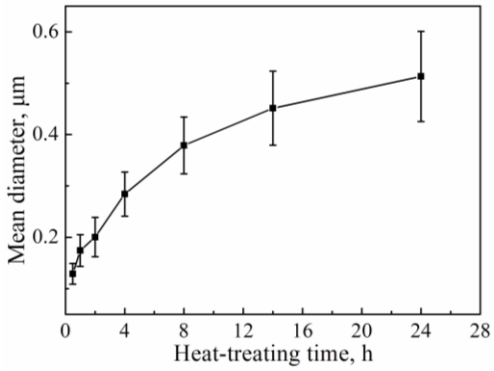

Fig. 4. Change of the mean diameter of droplets in cast stones as a function of heat-treating time. Error bars represent standard deviations.

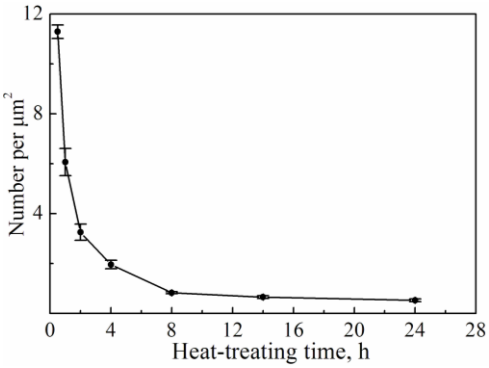

Fig. 5. Change of the number of droplets in cast stones as a function of heat-treating time. Error bars represent standard deviations.

3.3 Micro-area element analysis

The chemical compositions of the droplet phase and matrix phase of cast stone T-8 were detected by EDAX and the results were shown in Fig. 6. The EDAX method is difficult to accurately detect the chemical compositions of such small droplets, but capable to semi-quantitatively measure and estimate the difference of the element contents between the droplet phase and surrounding matrix phase. The result reveals that the droplet phase is rich in Ca and P, while the matrix phase rich in Si and F, in accordance with those investigated in the references [7-9], indicating that the element enrichment arose and thus resulted in the phase separation in the procedure of heat-treating the precursor into cast stone.

4. Discussion

4.1 The mechanism of phase separation

Two mechanisms of phase separation have been widely studied and well accepted by researchers:

spinodal decomposition in the region of the absolutely unstable states of the phase diagram and binodal decomposition (a nucleation and growth process) in the region of the metastable states [7,10-13]. The microstructures of two phase separation mechanisms are quite different. For the spinodal decomposition, a second phase with a highly connected structure is usually separated. In contrast, for the binodal decomposition, a discrete spherical phase generally precipitates and imbeds individually in the matrix phase. In this study, the chemical composition of the precursor of PS cast stone given in Table 2 locates in the metastable region of CaO-Al_2O_3-SiO_2 phase diagram [14], and the microstructure of the resulting cast stone observed in Fig. 2 is well consist with that generated by the binodal decomposition. Therefore, the phase separation occurred during heat-treating the precursor into cast stone is a typical one governed by the binodal decomposition.

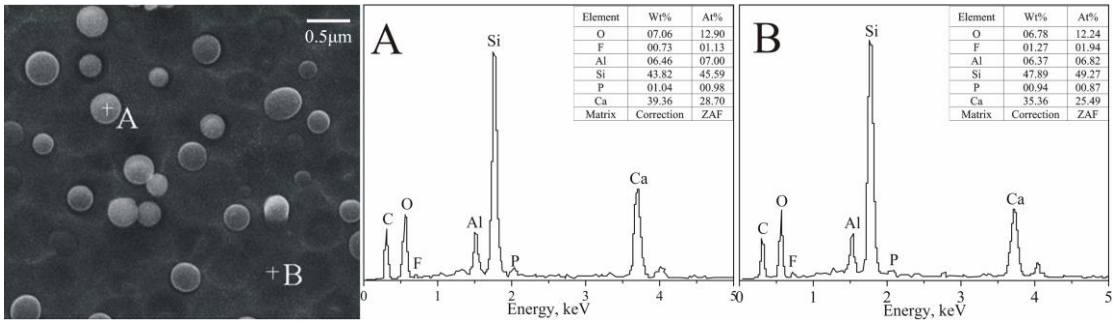

Fig. 6. EDAX spectra of (A) droplet phase and (B) matrix phase of cast stone T-8.

According to the thermodynamics of the binodal decomposition [13], the second differential of Gibbs free energy versus composition relationship $(\delta^2G/\delta C^2)_{T,P}$ is positive, and thus a small composition fluctuation will lead to an increase of the free energy. In this case, although the glass system located in the metastable region with a very low supersaturation tends to phase-separate, there exists a nucleation barrier and needs the outside energy to overcome it. Obviously, the heat treatment can continuously provide the energy for the precursor to overcome nucleation barrier and thus promote it to phase separate and to finally precipitate the stable droplet phase.

4.2 The growth kinetics of droplet phase

It was simulated on the functional relationship between the mean diameter of droplets and heat-treating time. The resulting regression line is shown in Fig. 7 and the regression equation is given as follows:

$$D = 0.946T^{\frac{1}{3}} - 0.0219 \qquad (1)$$

where D is the mean diameter of droplets and T is the heat-treating time. It can be clearly seen that the mean diameter of droplets is directly proportional to the cube root of the heat-treating time. In addition, the droplets increase in size and decrease in number with the increase of heat-treating time as observed from Fig. 4 and Fig. 5. Therefore, it can be concluded that the growth of droplets primarily conforms to the theory of *Ostwald ripening* [15-17].

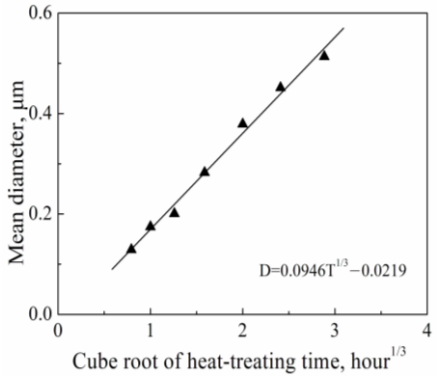

Fig. 7. The relationship of mean diameter of droplets in cast stones to the cube root of heat-treating time.

The growth of the precipitated droplets dominated by Ostwald ripening can be attribute to the diffusion of droplets in the matrix phase drove by the difference in the chemical potentials of droplets [18,19]. Chemical potential is described by Kelvin equation [20]:

$$c_{(r)} = c_{\infty}\exp\left[\frac{2\sigma M}{\rho_d rRT}\right] \qquad (2)$$

where c_∞ is the solubility of the droplet phase in the matrix phase; σ, M and ρ_d are respectively interfacial tension, molar mass and density of the droplet phase; r is droplet radius; R and T are gas constant and temperature.

During heat-treating the precursor into cast stone, because c_∞, M, ρ_d, R and T can be supposed as constants due to the invariable composition of droplets at a fixed temperature [13], the droplet radius r and interfacial tension σ affect greatly the chemical potentials of droplets. Clearly, the smaller droplet has higher chemical potential due to its small radius and high interfacial tension. Therefore, the difference of chemical potentials among neighboring droplets will drive the smaller droplets to coalesce and agglomerate into the bigger droplets, and thus the smaller disappears and the bigger grows, finally forming the droplets with a bigger and bigger size, as schematically described in Fig. 8.

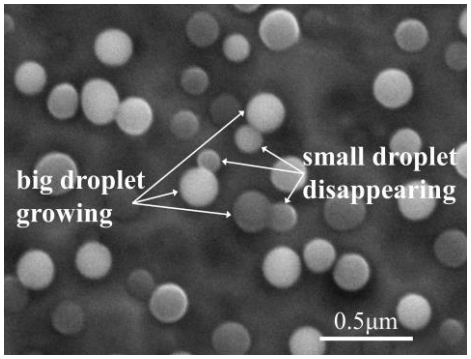

Fig. 8. The schematic growth process of droplets.

Obviously, this growth model will result in the droplet grains continuously increasing in size and decreasing in number as revealed in Figs. 4 and 5, which helps to reduce the surface energy of the droplets and the Gibbs free energy of the whole system to finally make them more stable [21, 22]. On the other hand, with the development of the droplets, the difference of the chemical potentials of droplets with the different sizes will tend to decrease, in return to restrain the growth rate of the droplets, which is reflected in the change tendency of the mean diameter of droplets versus heat-treating time as presented in Fig. 4.

4.3 The structural reason of phase separation

The chemical composition of the cast stone prepared mainly by PS belongs to CaO-Al_2O_3-SiO_2 system with small amounts of phosphorus (P) and fluorine (F). Both P_2O_5 and SiO_2 are network formers. In view of structural chemistry, the ionic field strength of P^{5+} ion (43.2) is higher than that of Si^{4+} ion (23.8) calculated by the formula $F=Z/r^2$ (F, ionic field strength; Z, ionic valence; r, ionic radius) [23-25]. Thus, P^{5+} ion can easily snatch oxygen from silicate network and form the phosphate network. The arrangement of PO_4 group in the silicate network was given in Fig. 9 [13]. The PO_4 group with one double bond (P=O) and three single bonds (P-O) is an asymmetric group, and thus causes the disturbance and disruption of the principal silicate network, leading to the precipitation of the droplet phase enriched with P, as observed from EDAX analysis (Fig. 6). At the same time, it is well known that fluorine can substitute for the bridging oxygen and bond preferentially with Si^{4+} [26-29], inevitably resulting in the disruption of the silicate framework and the reduction of the viscosity. Obviously, the disruption of network induced by P and F will form a short range framework different from the principle silicate network, which acts as the evocator of nucleation in the process of phase separation governed by the mechanism of binodal decomposition, and to a certain extent, promotes the phase separation of the precursor.

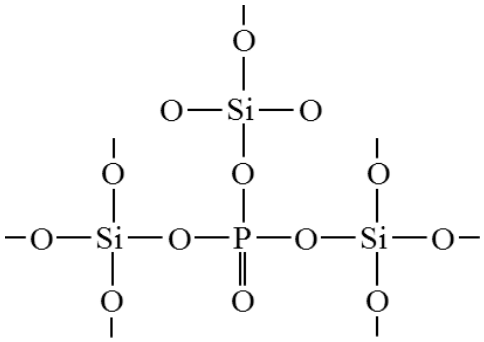

Fig. 9. The schematic arrangement of PO_4 groups in the silicate network.

5. Conclusion

The phase separation phenomenon and mechanism during heat-treating the precursor into the cast stone can be concluded as follows:

1. The XRD, FESEM and EDAX analyses revealed that, during being heat treated, the precursor underwent glass-in-glass phase separation with the precipitation of droplet phase rich in P and Ca from the matrix phase.

2. The microstructures of the as-obtained cast stones exhibit large quantities of droplets imbedding discretely in the matrix phase, signifying that the phase separation occurred in the course of heat-treating precursor is mainly governed by the mechanism of binodal decomposition.

3. The droplets increase in size and decrease in number with the increase of heat-treating time, and the mean diameter of droplets is linearly related to the cube root of the heat-treating time, implying that the growth kinetics of droplets primarily conforms to the theory of Ostwald ripening.

4. The growth of the droplets is achieved by coalescence and agglomeration of neighboring droplets drove by difference of chemical potentials.

5. A structural reason of phase separation is that the disturbance and disruption of the principle silicate network induced by P and F and the resulting short range

framework can act as an evocator of the phase separation.

Acknowledgement

The research work was financially supported by National Natural Science Foundation of China (No. 41002124).

References

[1] L. Cheng, C. Zhu, G. H. Sheng, J. Chin. Ceram. Soc. **34**, 604 (2006).
[2] B. Xu, K. M. Liang, J. W. Cao, Y. H. Li, Chin. Ceram. Commun. **105-106**, 600 (2010).
[3] G. R. Zhao, Y. Gao, Y. X. Li, A. G. Zheng, X. M. Kang, Concr. 84 (2011).
[4] O. E. Lebedeva, A. E. Dubovichenko, O. I. Kotsubinskaya, A. G. Sarmurzina, J. Non-Cryst. Solids **277**, 10 (2000).
[5] D. M. Liu, Mater. Comput. Mech. **117-119**, 1437 (2012).
[6] J. Zhou, Z. Shu, X. H. Hu, Y. X. Wang, Constr. Build. Mater. **24**, 811 (2010).
[7] A. Rafferty, R. G. Hill, D. Wood, J. Mater. Sci. **38**, 2311 (2003).
[8] C. Jana, W. Holand, Silic. Indus. **56**, 215 (1991).
[9] C. Moisescu, C. Jana, C. Russel, J. Non. Cryst. Solids **248**, 169 (1999).
[10] K. P. O'Flynn, K. T. Stanton, Cryst. Growth Des. **12**, 1218 (2012).
[11] M. C. Weinberg, V. A. Shneidman, Z. A. Osborne, Phys. Chem. Glasses **37**, 49 (1996).
[12] V. V. Golubkov, V. L. Stolyarova, Glass Phys. Chem. **37**, 252 (2011).
[13] P. W. McMillan, Glass-ceramics, Academic Press, New York, 1979.
[14] W. H. Jiang, Q. L. Liao, J. Chin. Ceram. Soc. **34**, 1356 (2006).
[15] P. Parthasarathy, A. V. Virkar, J. Power Sources **234**, 82 (2013).
[16] Y. Tang, G. Y. Li, Y. C. Pan, J. Alloys Compd. **554**, 195 (2013).
[17] D. Zhu, K. Li, X. Chen, T. Ying, Optoelectron. Adv. Mater.- Rapid Comm. **5**, 403 (2011).
[18] E. R. Garrett, J. Pharm. Sci. **51**, 811 (1962).
[19] E. Nazarzadeh, T. Anthonypillai, S. Sajjadi, J. Colloid Interface Sci. **397**, 154 (2013).
[20] L. M. Skinner, J. R. Sambles, J. Aerosol Sci. **3**, 199 (1972).
[21] A. K. Varshneya, Fundamentals of Inorganic Glasses, Academic Press, San Diego, 1994.
[22] I. M. Lifshitz, V. V. Slyozov, J. Phys. Chem. Solids **19**, 35 (1961).
[23] L. Luo, J. Z. Li, J. Non-Cryst. Solids **112**, 215 (1989).
[24] M. Arbab, V. K. Marghussian, H. Sarpoolaky, M. Kord, Ceram. Int. **33**, 943 (2007).
[25] X. F. Chen, L. L. Hench, D. Greenspan, J. P. Zhong, X. K. Zhang, Ceram. Int. **24**, 401 (1998).
[26] E. Y. Guseva, M. N. Gulyukin, Inorg. Mater. **38**, 962 (2002).
[27] K. Stanton, R. Hill, J. Mater. Sci. **35**, 1911 (2000).
[28] K. Sujirote, R. D. Rawlings, P. S. Rogers, J. Eur. Ceram. Soc. **18**, 1325 (1998).
[29] L. Bih, S. Mohdachi, A. Nadiri, M. Mansouri, M. Amalhay, O. Mykajlo, D. Kaynts, Optoelectron. Adv. Mater.- Rapid Comm. **2**, 253 (2008).

*Corresponding author: zhoujun@cug.edu.cn